

GENERATION OF MESOSTRUCTURE FOR LATTICE DISCRETE PARTICLE MODEL

JAN VOZÁB^{a,*}, JAN VOREL^a, MARCO MARCON^b, JAN PODROUŽEK^c,
ROMAN WAN-WENDNER^d

^a Czech Technical University in Prague, Faculty of Civil Engineering, 166 29 Prague 6, Czech Republic

^b University of Natural Resources and Life Sciences (BOKU), Department of Civil Engineering and Natural Hazards, Christian Doppler Laboratory LiCRoFast, 1190 Vienna, Austria

^c Brno University of Technology, Faculty of Civil Engineering, 602 00 Brno, Czech Republic

^d Ghent University, Laboratory for concrete research, 9052 Ghent, Belgium

* corresponding author: jan.vozab@fsv.cvut.cz

ABSTRACT. A preliminary study of two approaches for the internal structure generation utilized in the lattice discrete particle models (LDPM) [1] is presented. The presented methods used for particle generation and placement are meant to capture the internal structure of materials realistically. The first approach governs the positioning of the generated spherical particles by a gradient field to mimic the casting process. The second approach considers the non-spherical shape of individual particles, i.e. ellipsoidal particles. Therefore, the grain size, angularity, and flakiness can be controlled to match the real grain distribution closely.

KEYWORDS: Internal structure, LDPM, PGGF-G, Voronoi cell.

1. INTRODUCTION

Concrete and particulate polymers are assumed to be homogeneous on larger scales, but they are considered heterogeneous at lower scales [2]. The material internal structure can be viewed as aggregates bonded together by the matrix (cement paste, epoxy, etc.). The aggregates vary in size according to the grain size curve. The failure of these materials is mainly around the grains in the mortar [3, 4]. Breakage through the grains occurs mainly in high-strength concretes [1]. In this paper, we put our attention on the discrete particle model, more specifically Lattice Discrete Particle Model (LDPM) introduced by Cusatis et al. [1]. The LDPM material model response is dependent on particle distribution, and thus multiple simulations are needed to provide credible results [5].

2. LDPM MODEL

To take into account the underlying material structure, we chose the LDPM [1], utilizing the structure created from individual grains and allowing fracture only between these grains. As input for structure generation, we have the specimen's geometry and the prescribed gradation curve, i.e. maximum and minimum aggregate sizes. The maximum aggregate size defines the higher bound of the sieve curve. In contrast, the minimum aggregate size defines its arbitrary lower cut-off, i.e. the diameter under which no particles are discretely generated and placed. Thus, the minimum aggregate size affects the refinement of the discrete mesh and the computational cost.

Particles on the edges of the specimen are generated first, followed by the generation of particles on

the faces. These points are uniformly distributed and have zero diameters. The result of this generation is shown in Fig. 1a. Next, the particles in the interior of the element are generated. The interior particles are generated before placement, following a grain size curve with a specific diameter until the sum of their volumes is greater than a predetermined value. This value will be high enough to be a good representation of the number of particles in the actual element, but at the same time not too high so that the generation of the structure is not too computationally demanding. In the next step, the particle centres are positioned throughout the specimen volume one by one (from the largest to the smallest). They are placed in a random position, and a possible overlapping is checked. If the overlapping occurs, a new position is generated. In Fig. 1b you can see the result of the generation and placement of particles in the element. When all particles are generated, the next step is to calculate their interconnection using Delaunay triangulation. This computational method finds the smallest distances between particles, and the result is the fundamental geometric objects in 3D, which are tetrahedrons. These are made up of the nearest four particles. In Fig. 1c you can see the resulting connections of the Delaunay triangulation. Then the formation of individual LDPM cells from the tetrahedrons is employed. Each tetrahedron, composed of four vertices, is decomposed into four parts, which belong to individual cells connected through the facets. These facets are the planes connecting centroid, centres of the tetrahedron edges and centres of the tetrahedron faces. The facets' points on a tetrahedron take into account the diam-

eters of connected particles since a more significant part of the tetrahedron belongs to the bigger particle. In Fig. 1d the tetrahedron with four particles that represent its vertices is presented. Fig. 1e shows a portion of the tetrahedron associated with a single cell. The individual parts of tetrahedrons around the particles are then used to assemble the resulting polyhedral cells (Fig. 1g). When all the polyhedral particles are formed, their interaction with each other must be determined through the facets created by the splitting of the tetrahedrons. Displacements and rotations of such adjacent particles form the discrete compatibility equations in terms of rigid body kinematics. At each cell facet, the mesoscale constitutive law is formulated such that it simulates cohesive fracture, compaction due to pore collapse, frictional slip and rate effect. For every single particle, equilibrium equations are finally formulated.

3. GRADIENT FIELD POSITIONING

The first change we made to the LDPM model was to investigate the effect of particle location on fracture location and development. When a concrete specimen is formed, the distribution of particles can change due to vibration and gravity in such a way that larger particles are more concentrated near one of the surfaces of the specimen [6, 7]. However, this distribution no longer corresponds to the random placement used in the original LDPM model. Therefore, we tried to influence the distribution when creating the structure and modified the algorithm of particle placement according to a gradient-based field [8]. Therefore, the particles are placed according to the intensity of the field, which leads to the positioning of larger particles along one side of the sample. The results of random and gradient-based particle placement procedures are shown in Fig. 2a and Fig. 2b, respectively. The blue particles have the largest diameter, and the red particles have the smallest diameter. Comparing Fig. 2a with Fig. 2b, it can be seen that when the particles are placed according to the intensity field, the larger particles are placed mainly on the left side of the sample. The influence of different particle placement is mainly manifested by the moderate change of the crack paths (Fig. 3). However, the resistance of the specimen during the loading is influenced minimally by using the current formulation of LDPM.

4. VORONOID PARTICLE GENERATION

The second procedure is utilized to investigate the effect of grain shape on the crack development of the sample. The generation of particles is changed, and their shape is also controlled. More specifically, rotating ellipsoids are employed instead of spherical particles to match the actual shapes of grains. Possible approximations of different particle shapes are shown in Fig. 4. In the presented paper, the Voropp library [9] is used to generate particles with predefined

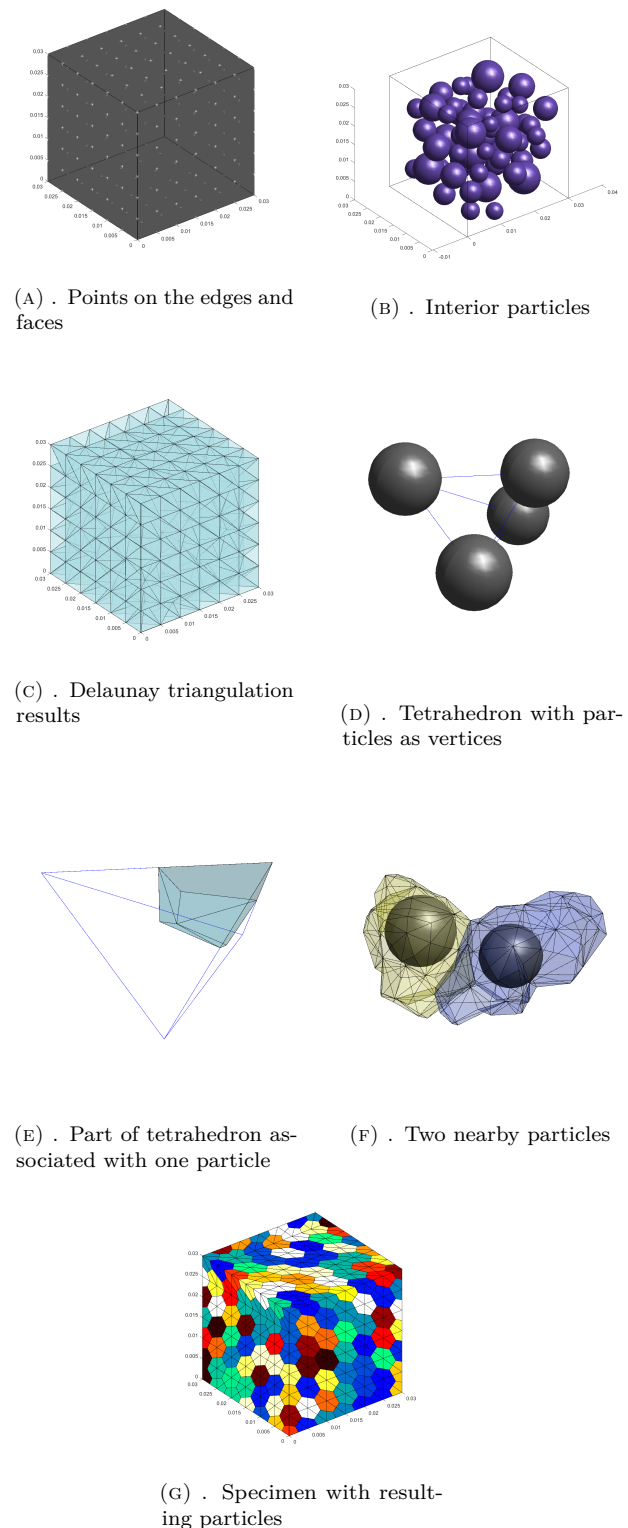
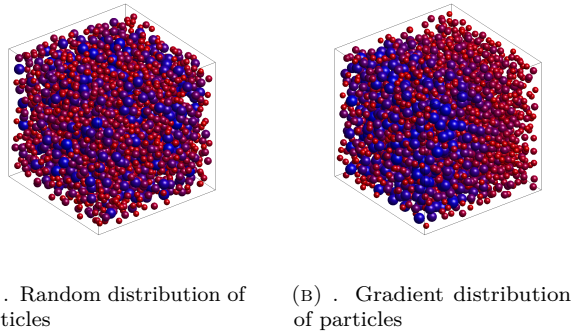


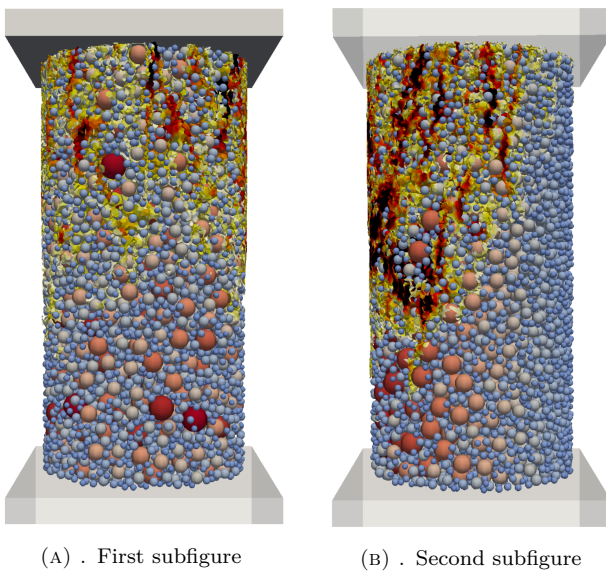
FIGURE 1. Generation of particles using LDPM.

shapes. The library allows the whole tessellations of particles. However, the current Voropp library only allows the generation of Voronoi diagrams for spherical particles. Creating the Voronoi cells for ellipsoidal particles is a complex task since the facets can be curved [10], and the cells are not necessarily convex [11]. This fact is illustrated in Fig. 5. Note that the effect of



(A) . Random distribution of particles (B) . Gradient distribution of particles

FIGURE 2. LDPM model, distribution of particles: (a) random distribution of particles; (b) gradient distribution of particles.



(A) . First subfigure (B) . Second subfigure

FIGURE 3. Results of the different particle distribution on the fracture propagation.

nonspherical particles is out of the scope of this paper and will be published separately.

5. CONCLUSION

The initial study of material structure effects on the location and development of cracks in a concrete specimen and similar type of materials is presented in the paper. Furthermore, a placement procedure taking into account the prescribed gradient field is described. According to the obtained results, changing the particle placement without affecting the material properties has a negligible effect on the response compared to the independent and random generation of particles. The description of the method, considering the nonspherical shape of particles, is also briefly described.

ACKNOWLEDGEMENTS

The financial support provided by the GAČR grant No. 21-28525S and by the Czech Technical University in Prague within SGS project with the application registered

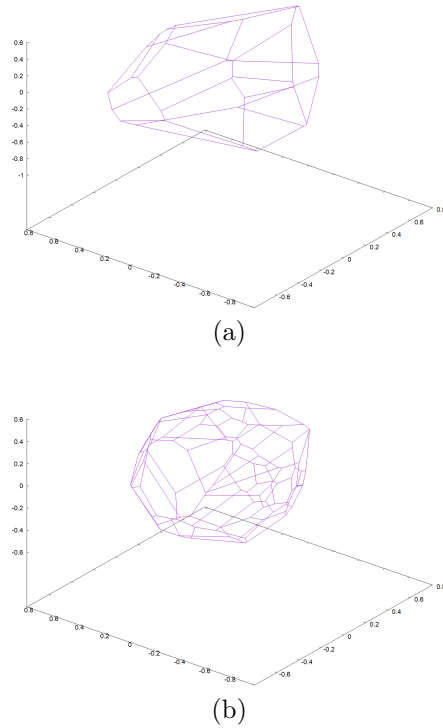


FIGURE 4. Concrete grains: (a) grain with higher flakiness index (elliptical); (b) cell with lower flakiness index (spherical).

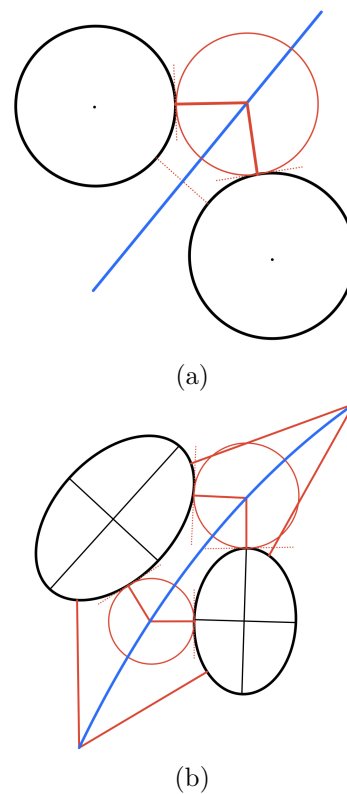


FIGURE 5. Generating boundary between particles: (a) circular particles; (b) elliptical particles.

under the No. SGS20/155/OHK1/3T/11 is gratefully acknowledged.

REFERENCES

- [1] G. Cusatis, D. Pelessone, A. Mencarelli. Lattice discrete particle model (ldpm) for failure behavior of concrete. i: Theory. *Cement and Concrete Composites* **33**(9):881–890, 2011.
- [2] N. Roussel. *Understanding the rheology of concrete*. Elsevier, 2011.
- [3] B. Karihaloo, A. Carpinteri, M. Elices. Fracture mechanics of cement mortar and plain concrete. *Advanced Cement Based Materials* **1**(2):92–105, 1993. [https://doi.org/10.1016/1065-7355\(93\)90014-F](https://doi.org/10.1016/1065-7355(93)90014-F).
- [4] K. Nagai, Y. Sato, T. Ueda. Mesoscopic simulation of failure of mortar and concrete by 3d rbsm. *Journal of Advanced Concrete Technology* **3**(3):385–402, 2005.
- [5] M. Marcon, J. Vorel, K. Ninčević, R. Wan-Wendner. Modeling adhesive anchors in a discrete element framework. *Materials* **10**(8):917, 2017.
- [6] Y. Peng, R. Lauten, K. Reknes, S. Jacobsen. Bleeding and sedimentation of cement paste measured by hydrostatic pressure and turbiscan. *Cement and Concrete Composites* **76**:25–38, 2017. <https://doi.org/10.1016/j.cemconcomp.2016.11.013>.
- [7] X. Gao, J. Zhang, Y. Su. Influence of vibration-induced segregation on mechanical property and chloride ion permeability of concrete with variable rheological performance. *Construction and Building Materials* **194**:32–41, 2019. <https://doi.org/10.1016/j.conbuildmat.2018.11.019>.
- [8] J. Podrouzek, J. Vorel, R. Wan-Wendner. Discrete particle placement schemes for ldpm. In *EMI International Conference*. Engineering Mechanics Institute (EMI), 2017.
- [9] C. Rycroft. Voro++: A three-dimensional voronoi cell library in c++. Tech. rep., Lawrence Berkeley National Lab.(LBNL), Berkeley, CA (United States), 2009.
- [10] I. Z. Emiris, E. P. Tsigaridas, G. M. Tzoumas. The predicates for the voronoi diagram of ellipses. In *Proceedings of the Twenty-Second Annual Symposium on Computational Geometry*, SCG '06, p. 227–236. Association for Computing Machinery, New York, NY, USA, 2006. <https://doi.org/10.1145/1137856.1137891>.
- [11] F. M. Schaller. The structure of random ellipsoid packings. 2012.